JACS
JOURNAL OF THE AMERICAN CHEMICAL SOCIETY
Cite This: J. Am. Chem. Soc. XXXX, XXX, XXX−XXX
Article
pubs.acs.org/JACS

Genetically Encoded Photocleavable Linkers for Patterned Protein Release from Biomaterials

Jared A. Shadish,[†] Alder C. Strange,[‡] and Cole A. DeForest*[,†,§,∥,⊥]

[†]Department of Chemical Engineering, [‡]Department of Biochemistry, and [⊥]Molecular Engineering & Sciences Institute, University of Washington, Seattle, Washington 98195, United States

[§]Department of Bioengineering, University of Washington, Seattle, Washington 98105, United States

[∥]Institute for Stem Cell & Regenerative Medicine, University of Washington, Seattle, Washington 98109, United States

Supporting Information

Given the critical role that proteins play in almost all biological processes, there is great interest in controlling their presentation within and release from biomaterials. Despite such outstanding enthusiasm, previously developed strategies in this regard result in ill-defined and heterogeneous populations with substantially decreased activity, precluding their successful application to fragile species including growth factors. Here, we introduce a modular and scalable method for creating monodisperse, genetically encoded chimeras that enable bioactive proteins to be immobilized within and subsequently photoreleased from polymeric hydrogels. Building upon recent developments in chemoenzymatic reactions, bioorthogonal chemistry, and optogenetics, we tether fluorescent proteins, model enzymes, and growth factors site-specifically to gel biomaterials through a photocleavable protein (PhoCl) that undergoes irreversible backbone photoscission upon exposure to cytocompatible visible light ($\lambda \approx 400$ nm) in a dose-dependent manner. Mask-based and laser-scanning lithographic strategies using commonly available light sources are employed to spatiotemporally pattern protein release from hydrogels while retaining their full activity. The photopatterned epidermal growth factor presentation is exploited to promote anisotropic cellular proliferation in 3D. We expect these methods to be broadly useful for applications in diagnostics, drug delivery, and regenerative medicine.

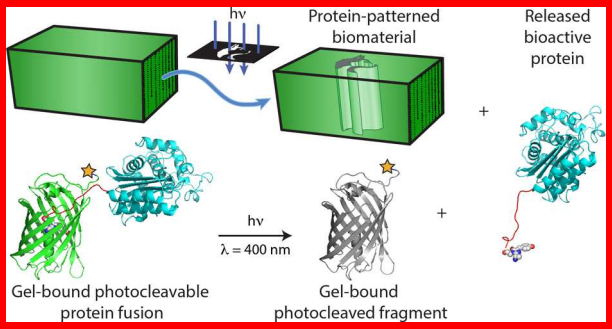

INTRODUCTION

Proteins represent the most functionally diverse class of biomolecules. Intimately involved in virtually all cellular signaling cascades and biological decisions of fate, there is long-standing interest in controlling their presentation within and release from biomaterials.[1−4] Though several chemical strategies exist to functionalize constructs indefinitely with biomacromolecules, "smart" materials that release proteins on demand have proven uniquely versatile in regulating therapeutic deployment and modulating cellular response in vitro and in vivo.[5,6] In one particularly powerful approach, proteins are covalently tethered to materials through degradable bonds; exposure to the appropriate preprogrammed stimulus induces bond cleavage and concomitant protein release.[7] Exploiting scissile moieties sensitive to pH, reductants, or enzymes, triggered protein release from 3D biomaterials has been demonstrated using a variety of biologically relevant external stimuli and for many different functional proteins.[8−12]

Although several stimuli-sensitive linkers have found utility in specifying *when* a protein payload is released, exceptionally few can also dictate *where* within a given material this occurs. Spatiotemporal control of protein release has unique utility in directing dynamic and anisotropic cell behaviors, and in serial therapeutic release.[13−16] Photochemical techniques are promising in this regard, enabling proteins to be released from materials with full 4D control.[17−19] Owing to their synthetic tractability and efficient photoscission under cytocompatible UV light, *ortho*-nitrobenzyl (*o*NB)- and coumarin (CM)-based esters have been the most commonly employed moieties for photomediated protein delivery.[20−24] Because *o*NB- and CM-based linkers are nonbiological and have not yet proven amenable to translational incorporation using genetic code expansion, postsynthetic strategies must be employed to install such photoactive species onto proteins.[25,26] Most commonly, activated esters of the photosensitive small molecules are coupled stochastically to primary amines present on lysine side chains and at the N-terminus, ultimately installing a variable number of photocleavable linkers through amide bonds at poorly defined locations on the protein surface. Though these approaches have been utilized to control 4D protein release, significant room for improvement exists because (1) postsynthetic chemical modification ensures a heterogeneous protein population that suffers from batch-to-batch variability and is likely intractable for translation, (2) random

Received: July 8, 2019

DOI: 10.1021/jacs.9b07239
J. Am. Chem. Soc. XXXX, XXX, XXX−XXX

modification with photoactive small molecules often results in substantially decreased protein bioactivity, and (3) the synthesis of *o*NB- or CM-modified photoreleasable proteins may be difficult to scale up.

Seeking to reap the benefits of phototriggered protein release while addressing the primary drawbacks of photosensitive small-molecule-based approaches, we envisioned tethering proteins of interest to biomaterials through a genetically encoded photocleavable protein known as PhoCl.[27] Recently developed by the optogenetics community as a unique tool for photoregulated gene expression, PhoCl is an engineered monomeric green fluorescent protein that undergoes irreversible β-elimination[28] and concomitant polypeptide backbone cleavage upon exposure to visible light ($\lambda \approx 400$ nm) (Scheme 1). The photocleavage of PhoCl yields

Scheme 1. Irreversible Photoscission and the Cleavage of PhoCl's Polypeptide Backbone[a]

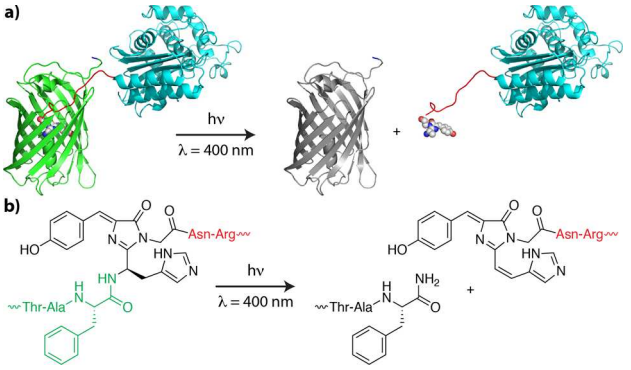

[a](a) Photocleavable fusion proteins undergo irreversible photoscission near PhoCl's C-terminus in response to cytocompatible violet light (λ = 400 nm), which is accompanied by PhoCl's loss of green fluorescence. The photoreleased protein of interest is shown in blue. (b) Photoinduced β-elimination of its matured chromophore results in the cleavage of PhoCl's polypeptide backbone.

a moderately sized N-terminal fragment (231 amino acids, 26 kDa) and a small C-terminal fragment (15 amino acids, 1.7 kDa), neither of which is fluorescent. Genetic fusions between PhoCl and proteins of interest can be recombinantly produced to yield perfectly defined photocleavable species using well-established and scalable fermentation processes.

To take advantage of the relatively small cleavage "scar" left on photoreleased proteins that had been fused C-terminally to PhoCl, we sought to immobilize the photoscissile chimeras to biomaterials through their N-terminus. In this regard, we identified N-myristoyltransferase (NMT), an enzyme which promotes cotranslational fatty acylation on proteins bearing the GXXXS/T signature peptide sequence (where X is any amino acid). Because NMT tolerates many synthetic analogs of its natural myristic acid substrate, including those containing azides, alkynes, carbonyls, and halogens,[29−31] we expected this to be a generalizable strategy compatible with many chemistries common to biomaterial formation and modification. Moreover, the efficiency and site-specificity of this chemoenzymatic transformation, coupled with NMT's cotranslational operation and the genetic encodability of all components, provide scalable access to perfectly defined chimeric proteins that can be precisely tethered to biomaterials and subsequently photoreleased upon visible light exposure.

RESULTS AND DISCUSSION

Toward the production of genetically encoded photoreleasable proteins, we created five expression vectors for PhoCl fused N-terminally with individual proteins from three distinct classes: mRuby, sfGFP, and mCerulean were selected for their fluorescence (red, green, and blue, respectively);[32−34] β-lactamase (bla) was included as a model enzyme; and epidermal growth factor (EGF) was chosen as a representative cytokine (Supporting Information Method S1). For each fusion construct, an NMT-recognition peptide sequence (MGNEASYPL)[35] and a 6xHis affinity purification tag were installed at PhoCl's N-terminus. *E. coli* was cotransformed with a single PhoCl fusion-containing plasmid and another encoding for NMT and methionine aminopeptidase,[36] enzymes essential for myristoylation. Because bioorthogonal click reactions involving reactive azides are now widely utilized in the synthesis and decoration of biomaterials,[37−40] we expressed proteins in the presence of 12-azidododecanoic acid (12-ADA) to site-specifically install a single azide to each protein through N-myristoylation (Scheme 2). Following

Scheme 2. NMT-Catalyzed Myristoylation of (a) PhoCl Fusions Bearing the N-Terminal GNEASYPL sequence with (b) 12-ADA Yields the Site-Specific Installation of the Azido Functionality

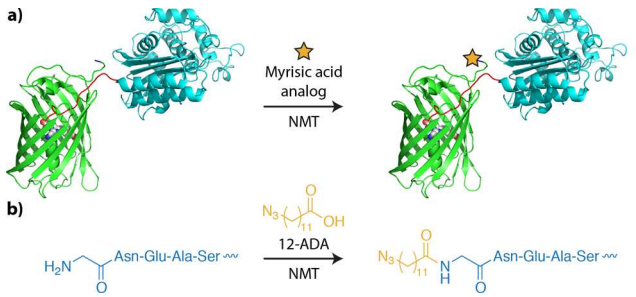

expression and affinity purification, the N-modified photoreleasable proteins were obtained in good yield (~15 mg L^{-1} culture, nonoptimized expression, Supporting Information Method S2). Analysis utilizing sodium dodecyl sulfate polyacrylamide gel electrophoresis (SDS-PAGE) and whole-protein mass spectrometry revealed high sample purity (>90%) and quantitative N-terminal azide-tagging (Supporting Information Figure S1, Supporting Information Method S3, Supporting Information Table S1).

To determine the photocleavage kinetics of the azide-modified chimeras, we investigated the PhoCl response to violet light (λ = 400 nm, 10 mW cm^{-2}, 0−30 min) for two different classes of proteins using independent methodologies. We first quantified the disappearance of N_3-PhoCl-bla fluorescence ($\lambda_{PhoCl,excitation}$ = 380 nm, $\lambda_{PhoCl,emission}$ = 510 nm) accompanying PhoCl photoscission at 25 °C (Supporting Information Figure S2). Under these conditions, PhoCl exhibited the expected first-order decay with a kinetic constant of 0.15 ± 0.02 min^{-1} and a half-life of 4.7 ± 0.6 min. To decouple photocleavage analysis from any potential photobleaching, SDS-PAGE analysis was subsequently performed on N_3-PhoCl-mRuby exposed to different amounts of light; the extent of photocleavage was determined by quantifying the intensities of the disappearing band from the intact fusion and the appearance of bands corresponding to the photocleaved products (Figure 1a,b). These analyses revealed a first-order

DOI: 10.1021/jacs.9b07239
J. Am. Chem. Soc. XXXX, XXX, XXX−XXX

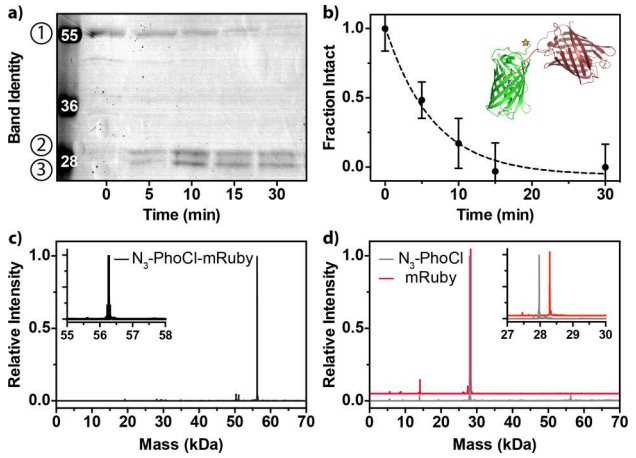

Figure 1. Validation and quantification of PhoCl photocleavage in response to violet light (λ = 400 nm, 10 mW cm^{-2}, 0–30 min). (a) SDS-PAGE analysis of N_3-PhoCl-mRuby exposed to different amounts of light, with band ① corresponding to the intact fusion, ② mRuby, and ③ PhoCl. Ladder-band molecular weights are given in kDa. (b) Normalized band intensity quantification yields the first-order decay constant. (c) Whole protein mass spectrometry indicates the high sample purity of N_3-PhoCl-mRuby. (d) Complete photocleavage of N_3-PhoCl-mRuby results in the scission of PhoCl's chromophore, yielding two distinct protein fragments with the expected mass. Error bars correspond to ±1 standard deviation about the mean for n = 3 experimental replicates.

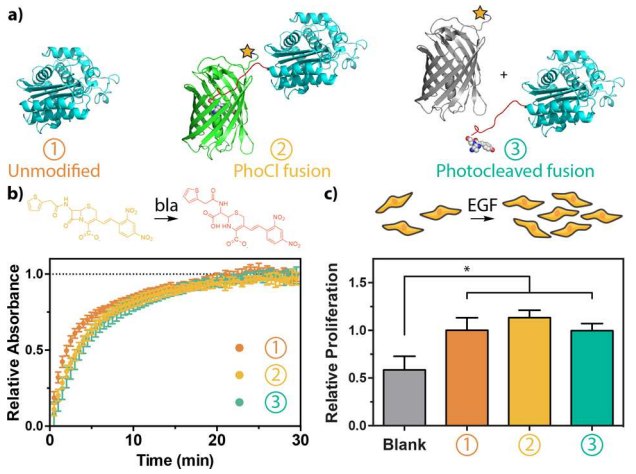

Figure 2. Intact and cleaved PhoCl fusions display native bioactivity. (a) Activities of the native protein were compared with the PhoCl chimera and its photocleaved products (denoted respectively by ①, ②, and ③). (b) Bla activity was determined by its ability to degrade a chromogenic nitrocefin substrate, which changes from yellow to red upon β-lactam cleavage. Time-course spectrophotometric analyses (λ_{abs} = 386 nm) indicate nitrocefin degradation for all species. (c) EGF bioactivity was determined on the basis of its ability to stimulate HeLa cell proliferation as quantified by increased dsDNA synthesis and content. Error bars correspond to ±1 standard deviation about the mean for n = 3 experimental replicates (*p < 0.05, unpaired two-tailed t test).

decay constant of 0.15 ± 0.03 min^{-1} and a half-life of 4.7 ± 0.8 min, values that were statistically indistinguishable from those based on the PhoCl fluorescence disappearance. To ensure that PhoCl cleaved at the expected location (PhoCl's H227 residue which matures as part of its chromophore), whole-protein mass spectrometry (ESI LC/MS) was performed on N_3-PhoCl-mRuby both before and after photocleavage (λ = 400 nm, 10 mW cm^{-2}, 30 min) (Figure 1c,d). Mass spectrometry revealed a singly azide-modified protein fusion of the expected mass (expected, 56.3 kDa; observed, 56.3 kDa) that decayed into the anticipated cleavage products (expected for PhoCl fragment, 28.0 kDa; observed for PhoCl fragment, 28.0 kDa; expected for mRuby fragment, 28.3 kDa; observed for mRuby fragment, 28.3 kDa) upon exposure to violet light.

Having determined the PhoCl domain's dose-dependent responsiveness to visible light, we next sought to compare the bioactivity of intact and photocleaved PhoCl fusions with the corresponding unmodified proteins of interest. Because spectral overlap and potential FRET between PhoCl and mRuby/sfGFP/mCerulean render fluorescence measurements a less-than-perfect surrogate for their retained bioactivity, we focused our efforts on the more fragile and biologically relevant bla and EGF proteins. Bla activity was assessed via a colorimetric assay involving the hydrolysis of the chromogenic cephalosporin nitrocefin, while EGF function was determined on the basis of its ability to stimulate HeLa cell proliferation as quantified by increased dsDNA synthesis and content (Supporting Information Methods S4–S5). In both cases, the activity of the native protein was statistically indistinguishable from that of the PhoCl fusion regardless of whether they had been photocleaved (λ = 400 nm, 10 mW cm^{-2}, 30 min) (Figure 2).

Encouraged that the genetically encoded photoreleasable proteins retained native bioactivity, we next sought to test their utility in a biomaterials context. Because the protein chimeras were N-terminally functionalized with reactive azides, we exploited hydrogel biomaterials formed via strain-promoted azide–alkyne cycloaddition (SPAAC) between poly(ethylene glycol) tetra-bicyclononyne (PEG-tetraBCN, M_n ≈ 20 kDa, 4 mM) and a linear PEG diazide (N_3-PEG-N_3, M_n ≈ 3.5 kDa, 8 mM) in phosphate-buffered saline (pH 7.4) (Supporting Information Method S6). Owing to the large water content of the resultant materials, a regular mesh size that supports soluble protein diffusion, and the bioorthogonal and cytocompatible nature of SPAAC,[41] these idealized step-growth polymer networks have proven beneficial for drug delivery and 3D cell culture applications.[42,43] Moreover, their optical clarity renders them useful constructs for photochemical modulation, particularly with respect to species photorelease. Finally, the inclusion of azide-tagged photocleavable fusion proteins during gel formulation facilitates their site-specific conjugation uniformly throughout biomaterials at user-defined concentrations.

To test to the potential utility of PhoCl fusions for photomediated protein delivery from biomaterials, N_3-PhoCl-sfGFP and N_3-PhoCl-bla were independently immobilized (15 μM) within SPAAC gels. A subset of each gel type was exposed to light (λ = 400 nm, 10 mW cm^{-2}, 30 min) to induce photocleavage. Sixteen hours after light exposure, gel supernatants were analyzed for soluble protein; sfGFP was quantified by its fluorescence ($\lambda_{sfGFP,excitation}$ = 488 nm, $\lambda_{sfGFP,emission}$ = 530 nm), while bla enzyme release was assessed using the colorimetric nitrocefin assay (Supporting Information Method S7). In both cases, supernatants of gels exposed to light indicated the successful phototriggered release of active proteins, whereas those from unexposed samples exhibited no nonspecific release (Figure 3). These experiments highlight the potential utility of this approach for on-demand protein

DOI: 10.1021/jacs.9b07239
J. Am. Chem. Soc. XXXX, XXX, XXX–XXX

therapeutic delivery as well as the strategy's absence of undesired leaky release.

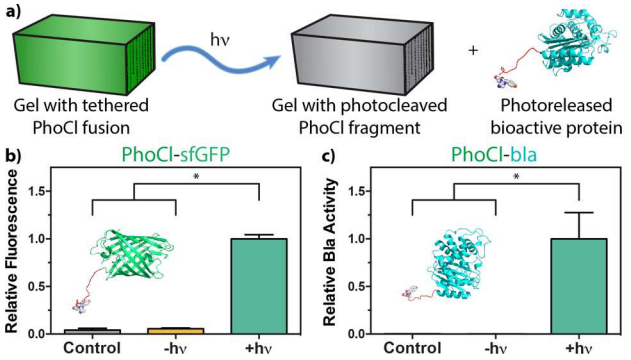

Figure 3. Proteins photoreleased from biomaterials remain active. (a) Photosensitive chimeras were tethered site-specifically to PEG-based hydrogels. Protein activity within the gel supernatant was assessed for PhoCl-containing samples kept in the dark or exposed to light (λ = 400 nm, 10 mW cm^{-2}, 30 min), as well as for control samples lacking protein. (b) Fluorescence measurements were utilized to assess sfGFP release. (c) A colorimetric nitrocefin assay was exploited to confirm functional bla release. Protein activities were normalized to light-treated condition results. Error bars correspond to ±1 standard deviation about the mean for n = 3 experimental replicates (*p < 0.05, unpaired two-tailed t test).

Because PhoCl cleavage can be spatiotemporally controlled using directed light, we sought to demonstrate its versatility in creating photopatterned protein-functionalized biomaterials. As a proof of concept, N_3-PhoCl-sfGFP, N_3-PhoCl-mRuby, and N_3-PhoCl-mCerulean (15 μM) were independently incorporated into PEG hydrogels during gelation. Protein-functionalized gels were then exposed to masked violet light (λ = 400 nm, 10 mW cm^{-2}, 30 min) to trigger PhoCl cleavage in user-defined patterns (tessellated geckos for sfGFP, squares for mRuby, and an Escher-inspired fish/bird pattern for mCerulean); released proteins were allowed to diffuse from the gels (16 h) prior to fluorescence confocal imaging ($\lambda_{sfGFP,excitation}$ = 488 nm, $\lambda_{sfGFP,emission}$ = 500−590 nm; $\lambda_{mRuby,excitation}$ = 560 nm, $\lambda_{mRuby,emission}$ = 600−700 nm; $\lambda_{mCerulean,excitation}$ = 405 nm, $\lambda_{mCerulean,emission}$ = 425−475 nm) (Figure 4a,b, Supporting Information Method S8, Supporting Information Figures S3 and S4). In each case, the fluorescence from the PhoCl domain colocalized with the fluorescent fusion partner. We anticipated this to be a convenient tool for tracking regions of protein immobilization should the protein of interest itself not be fluorescent. Results demonstrated micrometer-scale patterning resolution with long-term stability (>2 weeks).

Though conventional mask-based photolithography proved useful in generating binary-patterned materials, we next sought to exploit PhoCl's dose-dependent photoresponsiveness to create gradients of immobilized proteins through spatially varied photorelease. Gels containing N_3-PhoCl-mRuby (15 μM) were exposed to linear gradients of light, created by moving an opaque photomask across the gel surface at a fixed rate during light exposure (λ = 400 nm, 10 mW cm^{-2}).[44] To modulate the slope of the graded light, the photomask velocity was varied (0.4 and 1.2 mm min^{-1}). After light treatment and diffusive removal of the released protein from the gel, the patterned materials were imaged using fluorescence confocal microscopy (Figure 4c). Gradient signatures for both PhoCl

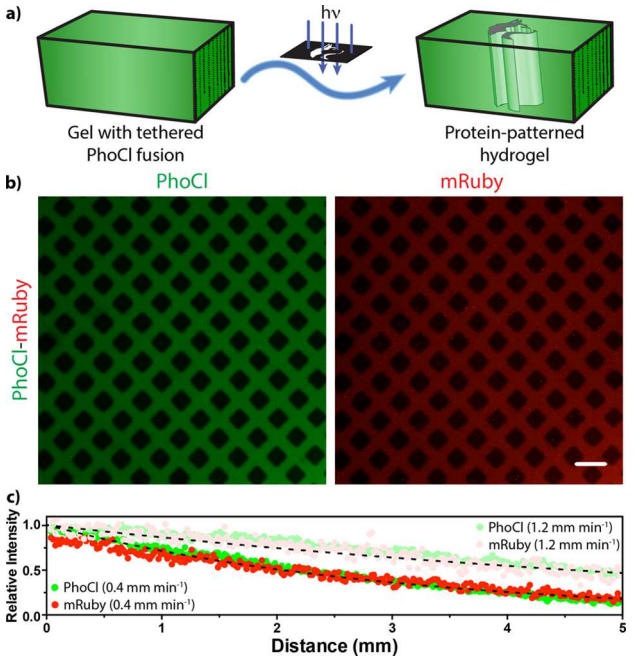

Figure 4. Protein-patterned gels generated using mask-based lithography. (a) Gels functionalized site-specifically with N_3-PhoCl-mRuby were exposed to masked violet light (λ = 400 nm, 10 mW cm^{-2}, 30 min) to trigger PhoCl cleavage in user-defined 2D patterns throughout the 3D gel thickness. (b) Fluorescence from PhoCl (green) colocalized with that from mRuby (red). Light-treated gel regions appeared black, owing to patterned photorelease of the fluorescent protein and PhoCl's cleavage-associated loss of fluorescence. Images correspond to a single z slice from stacks acquired by fluorescence confocal microscopy. Scale bar = 200 μm. (c) By subjecting hydrogels modified with N_3-PhoCl-mRuby to a linear gradient of light exposure (λ = 400 nm, 10 mW cm^{-2}), well-defined gradients of protein photorelease are achieved across relatively large distances. The slope of resultant protein gradient is readily controlled by tuning that of the light, here by adjusting the velocity by which an opaque photomask is translated over the gel (0.4 and 1.2 mm min^{-1}). Plots correspond to PhoCl and mRuby fluorescence intensity along the direction of photomask translation.

and mRuby fluorescence scaled as expected between the different graded light treatments and matched predictions from in-solution photocleavage kinetic analysis (Figure 1) with first-order decay with a kinetic constant of 0.15 ± 0.01 min^{-1} and a half-life of 4.6 ± 0.3 min. This precise control over protein release represents a powerful and facile tool for the creation of well-defined protein-patterned biomaterials.

Although PhoCl cleavage can be readily controlled using mask-based photolithography, we hypothesized that the overlap in wavelength emitted from a commonly available 405 diode laser (λ = 405 nm) with that required for photocleavage would render it amenable to laser-scanning lithographic patterning.[45−47] Here, hydrogels containing N_3-PhoCl-mCerulean (15 μM) were selectively exposed to focused laser light (λ = 405 nm) in user-defined regions of interests (ROIs) using a conventional confocal microscope (Supporting Information Method S8). Experiments revealed that tethered proteins could be completely released under mild laser conditions (5% laser power, scan speed = 200 Hz, 64 scan repeats, 10× objective, 100 mW 405 nm diode laser) (Supporting Information Figure S5). Moreover, because protein release scaled with photonic dosage, stepped protein

DOI: 10.1021/jacs.9b07239
J. Am. Chem. Soc. XXXX, XXX, XXX−XXX

gradients with micrometer-scale resolution could be generated by varying the number of laser scans (0−64) within adjacent regions of interest (Figure 5). Because diode laser lines and

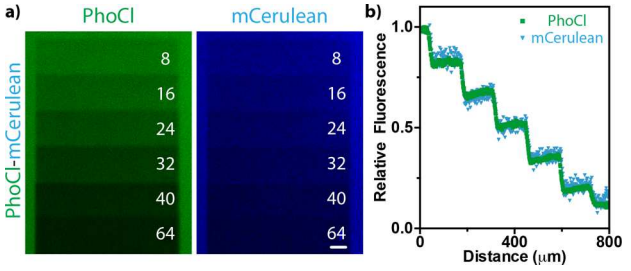

Figure 5. Protein-patterned gels generated through laser-scanning lithography. (a) Gels containing tethered N_3-PhoCl-mCerulean were selectively exposed to rastered laser scanning using a 405 nm diode laser line (100 mW laser, 5% laser power, scan speed = 200 Hz, 10× objective) with varied scan repeats (0−64) for different regions within a single imaging window, and stepped protein gradients were generated. Scale bar = 50 μm. (b) Plots correspond to the PhoCl and mCerulean fluorescence intensity along the gradient in (a).

controlled ROI scanning are common features on most confocal microscopes, arbitrarily patterned biomaterials can be generated within minutes using equipment that is readily available in virtually all academic research environments.

Having established the ability to modulate biomaterial properties with photoreleasable bioactive proteins, we investigated the effects of patterned EGF on cell fate. HeLa cells were encapsulated within the SPAAC-based gels containing an individual photosensitive chimera (4 μM); N_3-PhoCl-EGF was included to potentially promote cell proliferation, and N_3-PhoCl-mRuby was utilized as a non-cell-stimulating control. Gels were cross-linked with an azide-flanked linear peptide (6 mM, N_3-GGRGDSPGGPQGIWG-QGK(N_3)-NH_2, Supporting Information Method S9) that was susceptible to enzymatic cleavage by cell-secreted matrix metalloproteases and that contained a cell-adhesive RGD motif. One day after encapsulation, gels were exposed to patterned violet light (λ = 400 nm, 10 mW cm^{-2}, 30 min) through a slitted photomask containing 400-μm-wide line features to selectively release EGF/mRuby. Light exposure had no significant effect on cell viability (Supporting Information Figure S6), similar to recent reports for near-UV light.[48] Cells were maintained in culture for a total of 14 days and then fixed, and their nuclei were stained with 4′,6-diamidino-2-phenylindole (DAPI) prior to fluorescence and bright-field imaging (Figure 6, Supporting Information Method S10). Areas with persistently immobilized EGF (as visualized by PhoCl fluorescence) displayed significantly larger spheroid growth and more cell density than those where EGF had been photoreleased (p < 0.05). As expected, control experiments involving mRuby yielded spheroids whose size did not vary throughout the patterned gel and were smaller than those in the released EGF regions. These results demonstrate that PhoCl-mediated gel patterning can be performed with high fidelity in the presence of and to govern the spatiotemporal fate of encapsulated cells.

CONCLUSIONS

In this article, we have introduced a robust and versatile method to immobilize proteins site-specifically to and then subsequently photorelease them from hydrogel biomaterials.

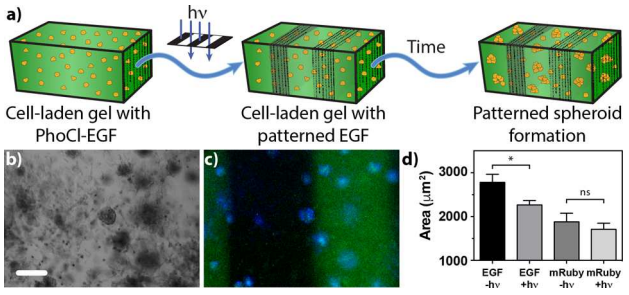

Figure 6. Controlling anisotropic cell proliferation through patterned EGF. (a) HeLa cells were encapsulated in gels uniformly functionalized with N_3-PhoCl-EGF or N_3-PhoCl-mRuby. After 1 day, proteins were photoreleased in line patterns (400-μm-wide features) using mask-based lithography. Cells were maintained in culture for a total of 14 days in the presence of the patterned protein prior to analysis. (b) Bright-field and (c) fluorescence confocal imaging (blue = nuclei, green = PhoCl-EGF) of EGF gels displays increased spheroid growth and a larger cell density in protein-tethered regions. Scale bars = 200 μm. (d) Image analysis illustrates a statistically significant variation in spheroid size in functionalized versus unfunctionalized regions for EGF gels but not for those containing patterned mRuby. Error bars correspond to ±1 standard deviation about the mean for n = 3 experimental replicates (*p < 0.05, unpaired two-tailed t test).

Relying on a cotranslational chemoenzymatic installation of a bioorthogonal reactive handle for N-terminal material tethering and the unique PhoCl protein that undergoes irreversible photoscission upon exposure to cytocompatible visible light, we control the immobilization and triggered delivery of fluorescent proteins, enzymes, and growth factors in a manner that preserves their activity. Because the entire system is genetically encoded, perfectly monodisperse photosensitive chimeras can be generated through scalable fermentation processes. Having demonstrated the spatiotemporally dictated release of bioactive species as well as the utility of photopatterned protein presentation toward guiding anisotropic cell fates in 3D, we anticipate that these approaches will find great utility in tissue engineering and therapeutic protein delivery.

ASSOCIATED CONTENT

Supporting Information

The Supporting Information is available free of charge on the ACS Publications website at DOI: 10.1021/jacs.9b07239.

General synthesis information, synthesis of previously reported compounds used in this work, Methods S1−S10, Figures S1−S6, and Table S1 (PDF)

AUTHOR INFORMATION

Corresponding Author

*profcole@uw.edu

ORCID

Jared A. Shadish: 0000-0003-1529-4286

Cole A. DeForest: 0000-0003-0337-3577

Notes

The authors declare no competing financial interest.

ACKNOWLEDGMENTS

The authors thank Dr. L. Newman and Dr. R. Kahn (Emory University) for gifting the hNMT1 with Met-AP plasmid,[36] as well as Dr. N. King for assistance with figure preparation. We

DOI: 10.1021/jacs.9b07239
J. Am. Chem. Soc. XXXX, XXX, XXX−XXX

gratefully acknowledge support from S. Edgar at the UW Mass Spectrometry Center as well as that from the NIH and N. Peters at the UW W. M. Keck Microscopy Center (S10 OD016240). This work was supported by a University of Washington Faculty Startup Grant (C.A.D.), a Jaconette L. Tietze Young Scientist Research Award (C.A.D.), and a CAREER Award (DMR 1652141, C.A.D.) from the National Science Foundation.

REFERENCES

(1) Hubbell, J. A. Bioactive Biomaterials. *Curr. Opin. Biotechnol.* **1999**, *10* (2), 123−129.
(2) Peppas, N. A.; Hilt, J. Z.; Khademhosseini, A.; Langer, R. Hydrogels in Biology and Medicine: From Molecular Principles to Bionanotechnology. *Adv. Mater.* **2006**, *18* (11), 1345−1360.
(3) Tayalia, P.; Mooney, D. J. Controlled Growth Factor Delivery for Tissue Engineering. *Adv. Mater.* **2009**, *21* (32−33), 3269−3285.
(4) Seliktar, D. Designing Cell-Compatible Hydrogels for Biomedical Applications. *Science* **2012**, *336* (6085), 1124−1128.
(5) Li, J.; Mooney, D. J. Designing Hydrogels for Controlled Drug Delivery. *Nat. Rev. Mater.* **2016**, *1*, 16071.
(6) Lu, Y.; Aimetti, A. A.; Langer, R.; Gu, Z. Bioresponsive Materials. *Nat. Rev. Mater.* **2016**, *1*, 16075.
(7) Badeau, B. A.; DeForest, C. A. Programming Stimuli-Responsive Behavior into Biomaterials. *Annu. Rev. Biomed. Eng.* **2019**, *21*, 241−265.
(8) Chen, W.; Zheng, M.; Meng, F.; Cheng, R.; Deng, C.; Feijen, J.; Zhong, Z. In Situ Forming Reduction-Sensitive Degradable Nanogels for Facile Loading and Triggered Intracellular Release of Proteins. *Biomacromolecules* **2013**, *14* (4), 1214−1222.
(9) Purcell, B. P.; Lobb, D.; Charati, M. B.; Dorsey, S. M.; Wade, R. J.; Zellars, K. N.; Doviak, H.; Pettaway, S.; Logdon, C. B.; Shuman, J. a; et al. Injectable and Bioresponsive Hydrogels for On-Demand Matrix Metalloproteinase Inhibition. *Nat. Mater.* **2014**, *13* (6), 653−661.
(10) Ham, H. O.; Qu, Z.; Haller, C. A.; Dorr, B. M.; Dai, E.; Kim, W.; Liu, D. R.; Chaikof, E. L. In Situ Regeneration of Bioactive Coatings Enabled by an Evolved Staphylococcus Aureus Sortase A. *Nat. Commun.* **2016**, *7*, 11140.
(11) Guo, C.; Kim, H.; Ovadia, E. M.; Mourafetis, C. M.; Yang, M.; Chen, W.; Kloxin, A. M. Bio-Orthogonal Conjugation and Enzymatically Triggered Release of Proteins within Multi-Layered Hydrogels. *Acta Biomater.* **2017**, *56*, 80−90.
(12) Gawade, P. M.; Shadish, J. A.; Badeau, B. A.; DeForest, C. A. Logic-Based Delivery of Site-Specifically Modified Proteins from Environmentally Responsive Hydrogel Biomaterials. *Adv. Mater.* **2019**, *31*, 1902462.
(13) Tibbitt, M. W.; Anseth, K. S. Dynamic Microenvironments: The Fourth Dimension. *Sci. Transl. Med.* **2012**, *4* (160), 160ps24.
(14) Burdick, J. A.; Murphy, W. L. Moving from Static to Dynamic Complexity in Hydrogel Design. *Nat. Commun.* **2012**, *3*, 1−8.
(15) DeForest, C. A.; Anseth, K. S. Advances in Bioactive Hydrogels to Probe and Direct Cell Fate. *Annu. Rev. Chem. Biomol. Eng.* **2012**, 3.421
(16) LeValley, P. J.; Kloxin, A. M. Chemical Approaches to Dynamically Modulate the Properties of Synthetic Matrices. *ACS Macro Lett.* **2019**, *8* (1), 7−16.
(17) Ruskowitz, E. R.; DeForest, C. A. Photoresponsive Biomaterials for Targeted Drug Delivery and 4D Cell Culture. *Nat. Rev. Mater.* **2018**, *3*, 17087.
(18) Sankaran, S.; del Campo, A. Optoregulated Protein Release from an Engineered Living Material. *Adv. Biosyst.* **2018**, *3*, 1800312.
(19) Rapp, T. L.; Highley, C. B.; Manor, B. C.; Burdick, J. A.; Dmochowski, I. J. Ruthenium-Crosslinked Hydrogels with Rapid, Visible-Light Degradation. *Chem. - Eur. J.* **2018**, *24* (10), 2328−2333.
(20) Griffin, D. R.; Schlosser, J. L.; Lam, S. F.; Nguyen, T. H.; Maynard, H. D.; Kasko, A. M. Synthesis of Photodegradable Macromers for Conjugation and Release of Bioactive Molecules. *Biomacromolecules* **2013**, *14* (4), 1199−1207.
(21) Azagarsamy, M. A.; Anseth, K. S. Wavelength-Controlled Photocleavage for the Orthogonal and Sequential Release of Multiple Proteins. *Angew. Chem., Int. Ed.* **2013**, *52* (51), 13803−13807.
(22) Wegner, S. V.; Sentürk, O. I.; Spatz, J. P. Photocleavable Linker for the Patterning of Bioactive Molecules. *Sci. Rep.* **2016**, *5* (1), 18309.
(23) DeForest, C. A.; Tirrell, D. A. A Photoreversible Protein-Patterning Approach for Guiding Stem Cell Fate in Three-Dimensional Gels. *Nat. Mater.* **2015**, *14* (5), 523−531.
(24) Shadish, J. A.; Benuska, G. M.; DeForest, C. A. Bioactive Site-Specifically Modified Proteins for 4D Patterning of Gel Biomaterials. *Nat. Mater.* **2019**, *18*, 1005−1014.
(25) Spicer, C. D.; Pashuck, E. T.; Stevens, M. M. Achieving Controlled Biomolecule−Biomaterial Conjugation. *Chem. Rev.* **2018**, *118* (16), 7702−7743.
(26) Fisher, S. A.; Baker, A. E. G.; Shoichet, M. S. Designing Peptide and Protein Modified Hydrogels: Selecting the Optimal Conjugation Strategy. *J. Am. Chem. Soc.* **2017**, *139* (22), 7416−7427.
(27) Zhang, W.; Lohman, A. W.; Zhuravlova, Y.; Lu, X.; Wiens, M. D.; Hoi, H.; Yaganoglu, S.; Mohr, M. A.; Kitova, E. N.; Klassen, J. S.; et al. Optogenetic Control with a Photocleavable Protein, PhoCl. *Nat. Methods* **2017**, *14* (4), 391−394.
(28) Mizuno, H.; Mal, T. K.; Tong, K. I.; Ando, R.; Furuta, T.; Ikura, M.; Miyawaki, A. Photo-Induced Peptide Cleavage in the Green-to-Red Conversion of a Fluorescent Protein. *Mol. Cell* **2003**, *12* (4), 1051−1058.
(29) Devadas, B.; Lu, T.; Katoh, A.; Kishore, N. S.; Wade, A. C.; Mehta, P. P.; Rudnick, D. A.; Bryant, M. L.; Adams, S. P.; Li, Q. Substrate Specificity of Saccharomyces Cerevisiae Myristoyl-CoA: Protein N-Myristoyltransferase. Analysis of Fatty Acid Analogs Containing Carbonyl Groups, Nitrogen Heteroatoms, and Nitrogen Heterocycles in an in Vitro Enzyme Assay and Subsequent Identifi. *J. Biol. Chem.* **1992**, *267* (11), 7224−7239.
(30) Heal, W. P.; Wright, M. H.; Thinon, E.; Tate, E. W. Multifunctional Protein Labeling via Enzymatic N-Terminal Tagging and Elaboration by Click Chemistry. *Nat. Protoc.* **2012**, *7* (1), 105−117.
(31) Kulkarni, C.; Kinzer-Ursem, T. L.; Tirrell, D. A. Selective Functionalization of the Protein N Terminus with N-Myristoyl Transferase for Bioconjugation in Cell Lysate. *ChemBioChem* **2013**, *14* (15), 1958−1962.
(32) Kredel, S.; Oswald, F.; Nienhaus, K.; Deuschle, K.; Röcker, C.; Wolff, M.; Heilker, R.; Nienhaus, G. U.; Wiedenmann, J. MRuby, a Bright Monomeric Red Fluorescent Protein for Labeling of Subcellular Structures. *PLoS One* **2009**, *4* (2), No. e4391.
(33) Pédelacq, J. D.; Cabantous, S.; Tran, T.; Terwilliger, T. C.; Waldo, G. S. Engineering and Characterization of a Superfolder Green Fluorescent Protein. *Nat. Biotechnol.* **2006**, *24* (1), 79−88.
(34) Rizzo, M. A.; Springer, G. H.; Granada, B.; Piston, D. W. An Improved Cyan Fluorescent Protein Variant Useful for FRET. *Nat. Biotechnol.* **2004**, *22* (4), 445−449.
(35) Kulkarni, C.; Lo, M.; Fraseur, J. G.; Tirrell, D. A.; Kinzer-Ursem, T. L. Bioorthogonal Chemoenzymatic Functionalization of Calmodulin for Bioconjugation Applications. *Bioconjugate Chem.* **2015**, *26* (10), 2153−2160.
(36) Van Valkenburgh, H. A.; Kahn, R. A. Coexpression of Proteins with Methionine Aminopeptidase and/or N-Myristoyltransferase in Escherichia Coli to Increase Acylation and Homogeneity of Protein Preparations. *Methods Enzymol.* **2002**, *344*, 186−193.
(37) Iha, R. K.; Wooley, K. L.; Nyström, A. M.; Burke, D. J.; Kade, M. J.; Hawker, C. J. Applications of Orthogonal "Click" Chemistries in the Synthesis of Functional Soft Materials. *Chem. Rev.* **2009**, *109* (11), 5620−5686.
(38) Nimmo, C. M.; Shoichet, M. S. Regenerative Biomaterials That "Click": Simple, Aqueous-Based Protocols for Hydrogel Synthesis, Surface Immobilization, and 3D Patterning. *Bioconjugate Chem.* **2011**, *22* (11), 2199−2209.

DOI: 10.1021/jacs.9b07239
J. Am. Chem. Soc. XXXX, XXX, XXX−XXX

(39) Azagarsamy, M. A.; Anseth, K. S. Bioorthogonal Click Chemistry: An Indispensable Tool to Create Multifaceted Cell Culture Scaffolds. *ACS Macro Lett.* **2013**, *2* (1), 5−9.
(40) Madl, C. M.; Heilshorn, S. C. Bioorthogonal Strategies for Engineering Extracellular Matrices. *Adv. Funct. Mater.* **2018**, *28* (11), 1706046.
(41) Agard, N. J.; Prescher, J. A.; Bertozzi, C. R. A Strain-Promoted [3 + 2] Azide-Alkyne Cycloaddition for Covalent Modification of Biomolecules in Living Systems. *J. Am. Chem. Soc.* **2004**, *126*, 15046−15047.
(42) DeForest, C. A.; Polizzotti, B. D.; Anseth, K. S. Sequential Click Reactions for Synthesizing and Patterning Three-Dimensional Cell Microenvironments. *Nat. Mater.* **2009**, *8* (8), 659−664.
(43) DeForest, C. A.; Anseth, K. S. Cytocompatible Click-Based Hydrogels with Dynamically Tunable Properties through Orthogonal Photoconjugation and Photocleavage Reactions. *Nat. Chem.* **2011**, *3* (12), 925−931.
(44) Johnson, P. M.; Reynolds, T. B.; Stansbury, J. W.; Bowman, C. N. High Throughput Kinetic Analysis of Photopolymer Conversion Using Composition and Exposure Time Gradients. *Polymer* **2005**, *46* (10), 3300−3306.
(45) Hahn, M. S.; Miller, J. S.; West, J. L. Laser Scanning Lithography for Surface Micropatterning on Hydrogels. *Adv. Mater.* **2005**, *17* (24), 2939−2942.
(46) DeForest, C. A.; Anseth, K. S. Photoreversible Patterning of Biomolecules within Click-Based Hydrogels. *Angew. Chem., Int. Ed.* **2012**, *51* (8), 1816−1819.
(47) Arakawa, C. K.; Badeau, B. A.; Zheng, Y.; DeForest, C. A. Multicellular Vascularized Engineered Tissues through User-Programmable Biomaterial Photodegradation. *Adv. Mater.* **2017**, *29* (37), 1703156.
(48) Ruskowitz, E. R.; DeForest, C. A. Proteome-Wide Analysis of Cellular Response to Ultraviolet Light for Biomaterial Synthesis and Modification. *ACS Biomater. Sci. Eng.* **2019**, *5* (5), 2111−2116.

DOI: 10.1021/jacs.9b07239
J. Am. Chem. Soc. XXXX, XXX, XXX−XXX